HAL open science

Tunable Exchange-Bias-Like Effect in Bi-Substituted Gadolinium Iron Garnet Film

Marwan Deb, Pierre Molho, Bernard Barbara

To cite this version:

Marwan Deb, Pierre Molho, Bernard Barbara. Tunable Exchange-Bias-Like Effect in Bi-Substituted Gadolinium Iron Garnet Film. Physical Review Applied, 2021, 15 (5), pp.054064. 10.1103/physrevapplied.15.054064 . hal-04158293

HAL Id: hal-04158293

https://hal.science/hal-04158293v1

Submitted on 11 Jul 2023

HAL is a multi-disciplinary open access archive for the deposit and dissemination of scientific research documents, whether they are published or not. The documents may come from teaching and research institutions in France or abroad, or from public or private research centers.

L'archive ouverte pluridisciplinaire **HAL**, est destinée au dépôt et à la diffusion de documents scientifiques de niveau recherche, publiés ou non, émanant des établissements d'enseignement et de recherche français ou étrangers, des laboratoires publics ou privés.

Tunable Exchange-Bias-Like Effect in Bi-Substituted Gadolinium Iron Garnet Film

Marwan Deb,[1,*] Pierre Molho,[2,3] and Bernard Barbara[2,3]

[1] *Institut für Physik und Astronomie, Universität Potsdam, Karl-Liebknecht-Str. 24-25, 14476 Potsdam, Germany*
[2] *CNRS, Institut Néel, F-38042 Grenoble, France*
[3] *Université Grenoble Alpes, Institut Néel, F-38042 Grenoble, France*

(Received 2 December 2020; revised 20 April 2021; accepted 10 May 2021; published 27 May 2021)

Using magneto-optical Faraday and Kerr measurements, we investigate the magnetic and magneto-optical properties of a thick Bi-substituted gadolinium iron garnet film over a broad range of wavelengths (250–850 nm) and temperatures (150–300 K), including the magnetization compensation point, T_M. We observe an exchange-bias-like effect in the vicinity of T_M. By slightly changing the sample temperature, we can precisely tune the bias field, which reaches a magnitude 6 times higher than the coercive field. We explain this phenomenon by considering the short-range superexchange interaction and a change in the magnetic behavior when moving from the surface to the bulk of the film. This finding may lead to the development of single-film magneto-optical devices based on the exchange-bias effect.

DOI: 10.1103/PhysRevApplied.15.054064

I. INTRODUCTION

Exchange bias (EB) is a magnetic phenomenon that manifests itself by a shift of the magnetic hysteresis loop along the field axis. This shift was discovered in 1956 by Mieklejohn and Bean in the ferromagnet (FM)-antiferromagnet (AF) system of core-shell Co/CoO nanoparticles [1] and phenomenologically related to the exchange interaction at the FM/AF interface, which creates a unidirectional magnetic anisotropy that alters the magnetization reversal of the FM layer. Since that time, EB has always been a very active research topic [2–6], in particular, due to its high potential impact for many technological applications, ranging from data-storage products [7,8] to spintronic devices [9–11], magnetic field sensors [12–16], and permanent magnet [17,18]. From a fundamental point of view, it provides an important opportunity to improve the understanding of surface and interface magnetism, which constitute a crucial issue in magnetic thin films and multilayers [2–6,19–23].

Most experimental and theoretical investigations of EB have been performed on FM/AF systems. However, over the years, EB was also observed in other types of interfaces involving a ferrimagnet (FI), as in FI/AF [24–26], FI/FM [7,27–29], and FI/FI [30,31] multilayers. Very recently, it was found that ferrimagnetic metallic films of Dy-Co showed an EB-like effect [32,33] associated with different bulk and surface magnetism, which are strongly coupled via exchange interactions. In this context, demonstrating the existence of an EB effect in a single FI insulator film of iron garnet is of utmost importance for both basic research and technological applications. Indeed, these garnets with large superexchange interactions [34] can also possess a significant perpendicular anisotropy, huge magneto-optical (MO) responses, and good optical transparency to visible and infrared light [34–37]. All these factors make them very suitable for magneto-optical recording and integrated optospintronic devices.

Here, we investigate the magnetic and magneto-optical properties of a thick Bi-substituted gadolinium iron garnet film by both Faraday and Kerr measurements over a broad range of wavelengths (250–850 nm) and temperatures (150–300 K). The sample, with perpendicular magnetic anisotropy much larger than the in-plane demagnetizing field, presents large MO responses, allowing us to demonstrate the existence of an exchange-bias-like effect near the compensation temperature, $T_M \sim 242$ K. By tuning the bias field, H_{EB}, through small changes to the temperature, we prove that it can be much higher than the coercive field ($H_{\mathrm{EB}} = 6.4 H_C$). We explain this EB-like phenomenon by considering a change in the magnetic behavior when moving from the surface to the bulk part of the film together with the atomic superexchange interaction.

II. SAMPLE PROPERTIES AND EXPERIMENTAL METHODS

The sample is a 7-μm-thick ferrimagnetic $(GdTmPrBi)_3(FeGa)_5O_{12}$ single-crystalline garnet film, grown by liquid-phase epitaxy (LPE) on a (111)-oriented gadolinium gallium garnet ($Gd_3Ga_5O_{12}$, GGG) substrate obtained

*madeb@uni-potsdam.de

 © 2021 American Physical Society

from CEA-LETI, France [38]. More information on the sample-growth conditions and the LPE system used can be found in Refs. [38,39]. The garnet film crystalizes in a centrosymmetric cubic structure with the space group $Pa\bar{3}d$, which is characterized by three different crystallographic sites (tetrahedral, octahedral, and dodecahedral) formed by the oxygen atoms [34,35]. These three crystallographic sites contribute to the magnetization of this material. The magnetic iron atoms are distributed over the nonequivalent tetrahedral and octahedral sites, which are coupled by a strong antiferromagnetic superexchange interaction. The noncompensated iron magnetic moment is coupled antiparallel to those of the rare-earth ions in the dodecahedral site by a much weaker superexchange interaction. Magnetization of the dodecahedral site comes mainly from Gd atoms, where a small amount of Pr is used to tune the magnetic anisotropy [38]. The exchange interaction within the Gd sublattice is very weak and magnetic ordering of the dodecahedral sublattice is mainly established by the strong negative exchange field induced by iron in the tetrahedral sublattice [34,35]. Due to the different temperature dependence of the antiferromagnetically coupled Gd and Fe magnetic moments, the net magnetization, M_S, of the film vanishes at the compensation temperature, T_M. The value of T_M is determined by the relative composition between Gd and Fe ions in the film and is estimated to be about 288 K in pure $Gd_3Fe_5O_{12}$ [40]. The nonmagnetic Bi and Ga ions are added to, respectively, improve the MO responses [41] and the optical transparency [42] of the film. A very small amount of Pb ions is also known to exist in dodecahedral sites in LPE garnets grown from PbO-based flux [41,43], as in the case of our film [38].

The magnetic and MO properties of the film are investigated using a custom-designed broadband MO spectrometer based on the 90°-polarization modulation technique [36,37]. Briefly, collimated white light emitted from a 150 W Xe arc lamp is polarized by a Rochon polarizer and modulated at 50 kHz with a Hinds photoelastic modulator (PEM). The modulated light is focused onto the sample at a near-normal incidence angle of 1.5°. The transmitted (resp. reflected) light is collimated and analyzed with a Rochon polarizer. The analyzed light is focused onto a monochromator equipped with a motorized filter wheel to eliminate higher-order diffraction and three diffraction gratings to cover the 200–2200 nm spectral range. The synchronous detection consists of a photomultiplier and two lock-in amplifiers at the fundamental and double PEM frequencies. The first-harmonic signal is proportional to the ellipticities (ε_F, ε_K), whereas the second-harmonic signal is proportional to the rotation (Θ_F, Θ_K). The sample is mounted in a helium-cooled magneto-optical cryostat with temperature stability better than 0.2 K. The external magnetic field, H_{ext}, can be applied perpendicular or parallel to the film plane.

III. RESULTS AND DISCUSSION

Figure 1 shows the spectral dependence of the MO Faraday and Kerr rotations (Θ_F, Θ_K) and ellipticities (ε_F, ε_K) measured at room temperature for a perpendicular saturating field, $H_{\text{ext}} = 8$ kA/m. Θ_F has a negative sign with a maximum of 3.9°/μm at 570 nm, whereas ε_F increases gradually when approaching the optical band gap ($E_g \approx 2.45$ eV). We note that the Faraday responses cannot be measured below this wavelength of 510 nm due to the large thickness of the studied film. Regarding the Kerr spectra, strong interference oscillations are observed between 510 and 750 nm for both Θ_F and ε_F. They reach a value of about 2.6° near 575 nm. Above the band gap, i.e., for $\lambda < 510$, Θ_K has two peaks with opposite signs and an equal amplitude of 0.66°, whereas ε_K reaches a maximum of 0.98° at 374 nm. The large Kerr signals and interferences below E_g are due to the multiple reflections in the film. Not surprisingly, the spectral dependencies of the Faraday and Kerr effects are in good agreement with previous studies of Bi-substituted iron garnet [36,37,44–47]. From a fundamental point of view, they are well explained in the visible and infrared regions by the crystal energy levels of Fe^{3+} ions in octahedral and tetrahedral symmetries

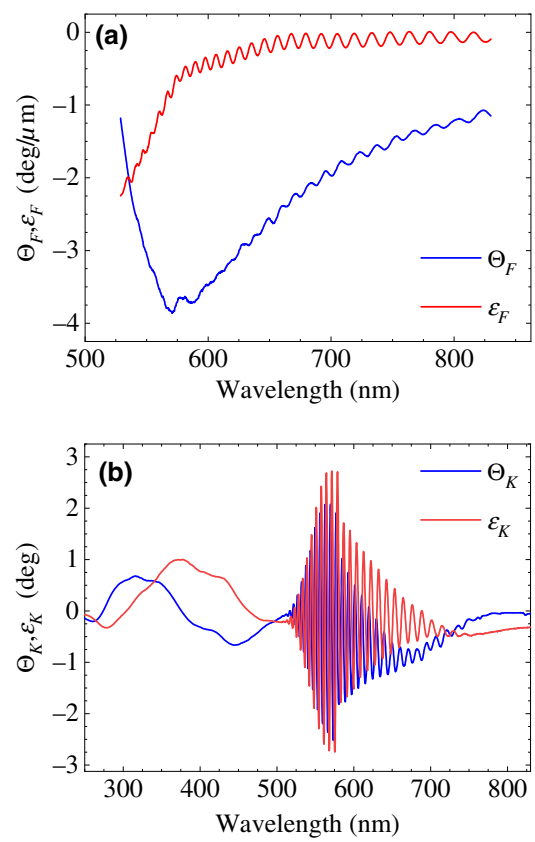

FIG. 1. Room-temperature magneto-optical polar (a) Faraday and (b) Kerr rotations (Θ_F, Θ_K) and ellipticities (ε_F, ε_K) of garnet film.

and their strong hybridization with the Bi $6p$ orbital, which is characterized by large spin-orbit coupling [46–49].

The temperature dependences of the magnetic and MO properties of the film are investigated by measuring the polar Kerr and Faraday hysteresis loops as a function of temperature [Figs. 2(a) and 2(b)]. The Faraday hysteresis loops reveal the magnetic properties of the entire sample, as transmitted light is analyzed. The Kerr hysteresis loops are measured at a wavelength of 450 nm, which is only sensitive to the first 1 ± 0.2 μm of the film. This value is estimated from an optical study performed on comparable samples with lower thickness. It is in good agreement with the one calculated from the penetration depth, δ_P, which is defined as the depth for which the intensity of light is reduced by a factor of $1/e$. Indeed, the Kerr signal stems primarily from about twice δ_P [50], which can be determined from the absorption coefficient, α, using the relationship $\delta_P = 1/\alpha$. The absorption coefficient at 450 nm in films with a composition of $YGdTmGa_{0.7}Fe_{2.3}O_{12}$, very similar to our garnet, is $\alpha = 1.8 \times 10^4$ cm^{-1} [51]. This gives $\delta_P = 0.55$ μm, and therefore, a thickness of about 1.1 μm can be probed via the Kerr effect. The normalized Kerr and Faraday hysteresis loops measured at 300 K are identical. The out-of-plane saturation field (~3 kA/m) is very small compared with the in-plane saturation one

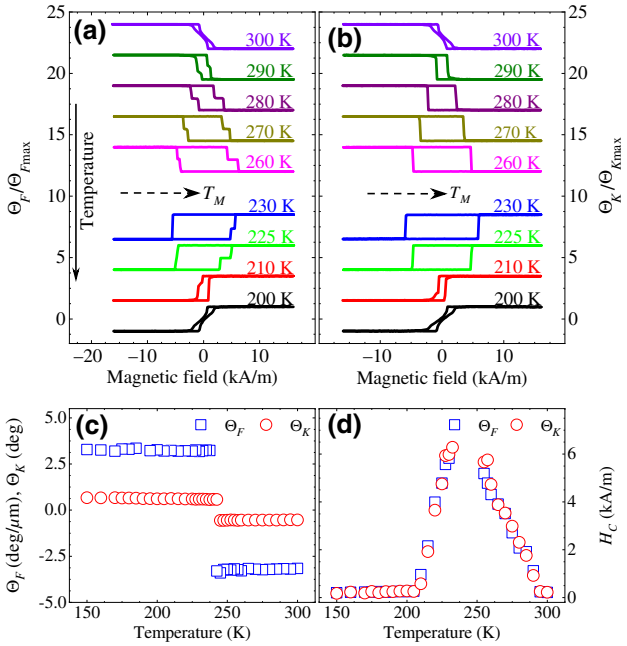

FIG. 2. Temperature dependence of magnetic and magneto-optical properties of garnet film measured with external magnetic field, H_{ext}, applied perpendicular to film plane. Normalized polar (a) Faraday and (b) Kerr hysteresis loops measured as a function of temperature. (c) Temperature dependences of Faraday rotation, Θ_F, and Kerr rotation, Θ_K, measured at wavelengths of 620 and 450 nm, respectively. (d) Temperature dependence of coercive field, H_C.

(160 kA/m, not shown), revealing strong perpendicular anisotropy. When decreasing the temperature from 300 to 260 K, the hysteresis loops become increasingly square and the coercive field, H_C, continuously increases. By further decreasing the temperature, the MO hysteresis loops change in sign and H_C decreases, as can be seen between 230 and 210 K. Below 205 K, the hysteresis loops revert to the nonsquare shape, as at 300 K [Figs. 2(a) and 2(b)].

To further illustrate the temperature dependence of the magnetic and MO properties, the amplitudes of Θ_F, Θ_K, and H_C are plotted as a function of temperature in Figs. 2(c) and 2(d). The absolute amplitudes of Θ_F and Θ_K have a very small or no dependence on temperature, which is in good agreement with the approach describing the MO effects in Bi-doped iron garnets with diamagnetic optical transitions [46,47,52]. On the other hand, near 242.5 K, both Θ_F and Θ_K change sign [Fig. 2(c)] and H_C maximizes [Fig. 2(d)]. Such behavior of H_C is typical at T_M. Indeed, to reverse magnetization, the applied energy field, $M_s H_C$, must overcome a constant magnetic energy barrier, and therefore, H_C increases significantly when M_S goes to zero [53–55]. The nonzero amplitude of the MO responses and their change of sign when crossing T_M are also common of ferrimagnets where the MO effects are dominated by the prevailing magnetic sublattice [46,47,52,56], and therefore, are not affected by the zero net value of M_S. Indeed, in Bi-substituted iron garnets, the MO signals in visible and infrared regions come from the resultant magnetization, M_{Fe}, of the Fe sublattices [46,47,52]. The change of M_s from being dominated by M_{Fe} to being dominated by M_{Gd} when crossing T_M leads to a reverse in the direction of M_{Fe} along H_{ext}, and therefore, to a change in the sign of the MO responses.

Interestingly, the Faraday and Kerr hysteresis loops measured between 235 and 250 K, i.e., closer to T_M, are more complex [Figs. 3(a) and 3(b)]. The Faraday ones show two important features. First, for magnetic fields higher than H_{EB}, the amplitude of Θ_F corresponds to a "pseudosaturated" state lower than the expected fully saturated state measured at the remanence. This pseudosaturated state is very stable and can be maintained up to 2800 kA/m. It is also observed in the ε_F hysteresis loops, confirming the magnetic origin of the phenomenon. Second, both H_{EB} and Θ_F ($H > H_{\text{EB}}$) highly depend on the temperature. At the compensation temperature, Θ_F ($H > H_{\text{EB}}$) tends to zero and H_{EB} minimizes, which is the opposite behavior of H_C [Figs. 3(a) and 3(d)]. Regarding the Kerr hysteresis loops, they show different, but nonetheless interesting, behavior. Indeed, at temperatures equal to or slightly lower than T_M, the hysteresis loops remain square with jumps at $\pm H_c$ without any further effect for $H_{\text{ext}} > H_c$. However, when the temperature becomes higher than T_M, a second hysteresis loop well separated from the main one appears at fields comparable to H_{EB} [Figs. 3(a) and 3(b)].

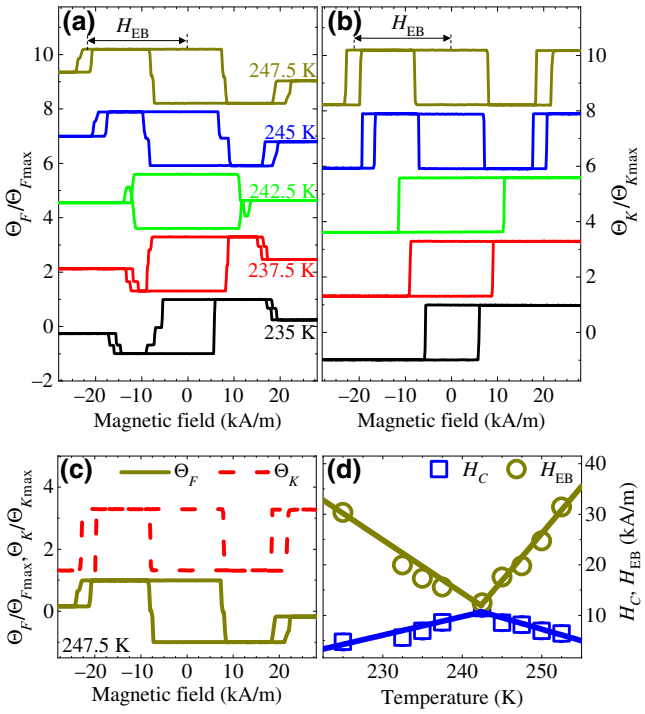

FIG. 3. Magnetic and magneto-optical properties of garnet sample in the vicinity of compensation temperature T_M. Normalized polar (a) Faraday and (b) Kerr hysteresis loops measured in vicinity of T_M. (c) Comparison between polar Faraday and Kerr hysteresis loops measured at 247.5 K. (d) Temperature dependence of coercive field H_C and exchange-bias field H_{EB}.

The square shape with the fully saturated state of the Kerr hysteresis loops near T_M reflects the high magnetic anisotropy of the film [see Fig. 3(b)]. This is in good agreement with the fact that near T_M the in-plane saturation field (∼160 kA/m) is still very high compared with that of the out-of-plane one (∼11 kA/m). Additionally, the abrupt reversal of Θ_K toward a fully saturated magnetic state for $H_{ext} > H_{EB}$ cannot be related to a spin-flop transition. Indeed, magnetization of the first 1 μm probed by the Kerr effect is always aligned with the direction of H_{ext}, whereas, for spin-flop transitions, all spins turn continuously from the normal of the sample (i.e., turn toward the direction perpendicular to H_{ext}), get canted, and form a noncollinear state [57–59].

To understand the observed Kerr and Faraday hysteresis loops and their complex shapes near T_M, we consider a composition gradient through the sample thickness, which leads to a continuous variation of T_M. This effect is not surprising in thick garnets films grown by LPE, where a decrease in the amount of incorporated Pb and Bi atoms usually occurs during growth [60,61], and therefore, fewer Gd atoms are substituted when the thickness of the crystal increases. This leads to a gradient of the compensation temperature across the film, which increases when approaching the surface. To describe this situation, we define three compensation temperatures for the behavior at the interface, T_{MI}; in the bulk, T_{MB}; and at the surface, T_{MS}, where $T_{MI} < T_{MB} \cong T_M < T_{MS}$. As a consequence, for temperatures between T_{MI} and T_{MB}, the atomic planes near the interface with GGG, which we call the "interface layer," will be dominated by M_{Fe}, whereas the rest of the film will be dominated by M_{Gd}. The individual behaviors of the interface layer and the rest of the film, as well as their interplay, should play a role in the measured hysteresis loops. On the other hand, for temperatures between T_{MB} and T_{MS}, the atomic planes near the surface, which we call the "surface layer," will be dominated by M_{Gd}, whereas the rest of the film will be dominated by M_{Fe}. In this case, the individual behaviors of the surface layer and the rest of the film, as well as their interplay, should play a role in the measured hysteresis loops. We denote in the following the rest of the film as "bulk," as it represents the thicker part of the film with the same net magnetization direction.

The Kerr and Faraday hysteresis loops measured at 247.5 K can be used to provide clear insights into the mechanisms behind the complex shapes of the observed hysteresis loops (Fig. 4). At this temperature, slightly above T_M, the atomic planes near the surface are dominated by M_{Gd}, whereas those of the bulk are dominated by M_{Fe}. At the magnetic remanence, the strong superexchange interactions couple the Fe spins of the surface layer to the bulk ones, leading to the spin configuration of Fig. 4(c), where the surface magnetization is antiparallel to the bulk one. At high fields, the Zeeman interaction becomes stronger than the exchange coupling and the net surface magnetization reverses to align parallel to the field direction. The reversal of the surface layer occurs at H_{EB} and leads to a modulated out-of-plane domain-wall configuration within the volume of the film, in which the anisotropy and exchange energy are stored [Fig. 4(d)]. This induces a decrease of the Faraday signal due to the transition of the surface Fe magnetic moments from parallel to antiparallel to H_{ext} [Fig. 4(b)]. The full reversal of the Kerr signal above H_{EB} [Fig. 4(a)] is related to the large thickness of the surface layer compared with the probed thickness by the Kerr effect. The same approach can also explain the complex hysteresis loops observed for temperatures slightly below T_M, i.e., $T_{MI} < T < T_{MB}$, where an interface layer is dominated by M_{Fe}, whereas the rest of the film is dominated by M_{Gd}. In this case, when the external field reaches H_{EB}, the net magnetization of the interface layer will rotate to align parallel to H_{ext}, while magnetization of the top part of the bulk remains unchanged, as it is already aligned with H_{ext} at H_C. The Faraday signal will therefore show a jump at H_{EB}, while no effect will appear in Kerr loops, as the deeply buried interface layer cannot be detected by the Kerr effect. We note that a study of the domain wall and magnetization profile inside a magnetic system can be performed using polarized-neutron reflectivity measurements [62–65]. Indeed, such a technique has

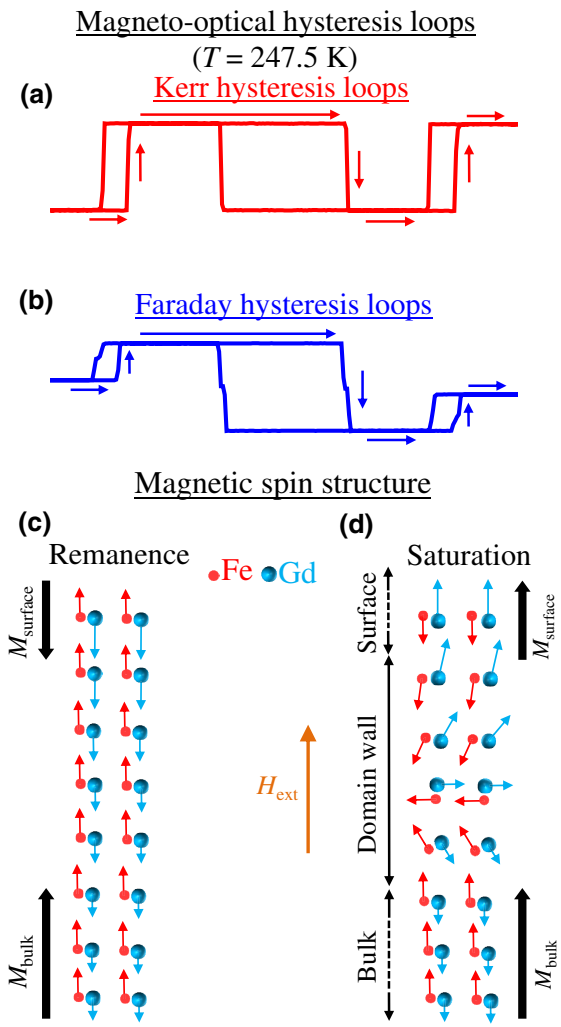

FIG. 4. Magnetic spin structure near T_M. Normalized polar (a) Faraday and (b) Kerr hysteresis loops measured at 247.5 K. Arrows show evolution of hysteresis loops as a function of external magnetic field. Sketch of magnetic spin structure of garnet film at 247.5 K in (c) remanent and (d) saturation magnetic states.

been previously used to predict an interfacial domain-wall formation in the ferromagnetic layer of exchange-coupled Fe_3O_4/NiO multilayers [65]. Such a full polarized-neutron study goes beyond the scope of the present paper.

The position of the domain wall is highly dependent on temperature. It is located closer to the substrate for temperatures $T_{MI} < T < T_{MB}$ and moves toward the surface by increasing the temperature above T_{MB}. The width of this out-of-plane domain wall, W_D, is given by $W_D = \pi\sqrt{A/K}$, where A and K are, respectively, the atomic exchange stiffness and the crystalline anisotropy of the film [66]. Using values of $A = 3.26 \times 10^{-7}$ erg/cm and $K = 10\,628$ erg/cm^3 obtained in films with similar compositions and anisotropy [67], a domain-wall width of $W_D = 174$ nm is obtained. On the other hand, H_{EB} can be expressed as $H_{EB} = 2\sqrt{AK}/t_s M_S$, where t_s and M_s are the thickness and saturation magnetization of the "surface" [66]. From the amplitude of the Faraday hysteresis loops for $H > H_{EB}$ [see Fig. 3(b)], we can safely assume $t_s \sim 2.9$ μm at 247.5 K. Moreover, near T_M, M_s should have a value of very few emu/cm^3. Using a value of $M_s = 1.5$ emu/cm^3 yields H_{EB} $(T = 247.5$ K$) \sim 270$ Oe, i.e., 21 kA/m, in agreement with experimental data.

IV. CONCLUSION

We investigate the magnetic and magneto-optical properties of a thick film of Bi-substituted gadolinium iron garnet by both Faraday and Kerr effects over a broad range of wavelengths (250–850 nm) and temperatures (150–300 K), including the compensation point, T_M. We show that the sample has a perpendicular magnetic anisotropy together with a large MO response, which fully fulfils the conditions for many magnetic and MO applications. In particular, we demonstrate an exchange-bias-like effect near T_M. We show that the bias field, H_{EB}, may be much larger than H_C $(H_{EB} = 6.4H_C)$, and we explain this phenomenon by considering a change in the magnetic behavior when moving from the surface to the bottom part of film. This large and tunable exchange-bias effect may lead to the development of single-film magneto-optical devices based on exchange bias.

ACKNOWLEDGMENTS

M.D. acknowledges the Alexander von Humboldt Foundation for financial support.

[1] W. H. Meiklejohn and C. P. Bean, New magnetic anisotropy, Phys. Rev. **102**, 1413 (1956).
[2] R. L. Stamps, Mechanisms for exchange bias, J. Phy. D: Appl. Phys. **33**, R247 (2000).
[3] F. Radu and H. Zabel, in *Magnetic Heterostructures: Advances and Perspectives in Spinstructures and Spintransport*, edited by H. Zabel, S. D. Bader (Springer Berlin Heidelberg, Berlin, Heidelberg, 2008), pp. 97.
[4] K. Yang, W. Paul, F. D. Natterer, J. L. Lado, Y. Bae, P. Willke, T. Choi, A. Ferrón, J. Fernández-Rossier, A. J. Heinrich, *et al.*, Tuning the Exchange Bias on a Single Atom From 1 mT to 10 T, Phys. Rev. Lett. **122**, 227203 (2019).
[5] P.-H. Lin, B.-Y. Yang, M.-H. Tsai, P.-C. Chen, K.-F. Huang, H.-H. Lin, and C.-H. Lai, Manipulating exchange bias by spin–orbit torque, Nat. Mater. **18**, 335 (2019).
[6] E. Lachman, R. A. Murphy, N. Maksimovic, R. Kealhofer, S. Haley, R. D. McDonald, J. R. Long, and J. G. Analytis, Exchange biased anomalous Hall effect driven by frustration in a magnetic kagome lattice, Nat. Commun. **11**, 560 (2020).
[7] S. Parkin, J. Xin, C. Kaiser, A. Panchula, K. Roche, and M. Samant, Magnetically engineered spintronic sensors and memory, Proc. IEEE **91**, 661 (2003).

[8] D. Suess, T. Schrefl, S. Fähler, M. Kirschner, G. Hrkac, F. Dorfbauer, and J. Fidler, Exchange spring media for perpendicular recording, Appl. Phys. Lett. **87**, 012504 (2005).

[9] A. V. Khvalkovskiy, D. Apalkov, S. Watts, R. Chepulskii, R. S. Beach, A. Ong, X. Tang, A. Driskill-Smith, W. H. Butler, P. B. Visscher, et al., Basic principles of STT-MRAM cell operation in memory arrays, J. Phys. D: Appl. Phys. **46**, 074001 (2013).

[10] T. Gasi, A. K. Nayak, J. Winterlik, V. Ksenofontov, P. Adler, M. Nicklas, and C. Felser, Exchange-spring like magnetic behavior of the tetragonal Heusler compound Mn_2FeGa as a candidate for spin-transfer torque, Appl. Phys. Lett. **102**, 202402 (2013).

[11] T. N. A. Nguyen, Y. Fang, V. Fallahi, N. Benatmane, S. M. Mohseni, R. K. Dumas, and J. Åkerman, [Co/Pd]–NiFe exchange springs with tunable magnetization tilt angle, Appl. Phys. Lett. **98**, 172502 (2011).

[12] M. N. Baibich, J. M. Broto, A. Fert, F. N. Van Dau, F. Petroff, P. Etienne, G. Creuzet, A. Friederich, and J. Chazelas, Giant Magnetoresistance of (001)Fe/(001)Cr Magnetic Superlattices, Phys. Rev. Lett. **61**, 2472 (1988).

[13] B. Dieny, V. S. Speriosu, S. Metin, S. S. P. Parkin, B. A. Gurney, P. Baumgart, and D. R. Wilhoit, Magnetotransport properties of magnetically soft spin-valve structures (invited), J. Appl. Phys. **69**, 4774 (1991).

[14] G. Malinowski, M. Hehn, M. Sajieddine, F. Montaigne, E. Jouguelet, F. Canet, M. Alnot, D. Lacour, and A. Schuhl, Using antiferromagnetic/ferromagnetic bilayers as detection layers in magnetic tunnel junctions, Appl. Phys. Lett. **83**, 4372 (2003).

[15] C. Chappert, A. Fert, and F. N. Van Dau, The emergence of spin electronics in data storage, Nat. Mater. **6**, 813 (2007).

[16] B. Negulescu, D. Lacour, F. Montaigne, A. Gerken, J. Paul, V. Spetter, J. Marien, C. Duret, and M. Hehn, Wide range and tunable linear magnetic tunnel junction sensor using two exchange pinned electrodes, Appl. Phys. Lett. **95**, 112502 (2009).

[17] E. F. Kneller and R. Hawig, The exchange-spring magnet: A new material principle for permanent magnets, IEEE Trans. Magn. **27**, 3588 (1991).

[18] J. Sort, J. Nogués, S. Suriñach, J. S. Muñoz, M. D. Baró, E. Chappel, F. Dupont, and G. Chouteau, Coercivity and squareness enhancement in ball-milled hard magnetic–antiferromagnetic composites, Appl. Phys. Lett. **79**, 1142 (2001).

[19] J. Nogués and I. K. Schuller, Exchange bias, J. Magn. Magn. Mater. **192**, 203 (1999).

[20] S. Giri, M. Patra, and S. Majumdar, Exchange bias effect in alloys and compounds, J. Phys.: Condens. Matter **23**, 073201 (2011).

[21] M. Kiwi, Exchange bias theory, J. Magn. Magn. Mater. **234**, 584 (2001).

[22] F. Hellman, A. Hoffmann, Y. Tserkovnyak, G. S. D. Beach, E. E. Fullerton, C. Leighton, A. H. MacDonald, D. C. Ralph, D. A. Arena, H. A. Dürr, et al., Interface-induced phenomena in magnetism, Rev. Mod. Phys. **89**, 025006 (2017).

[23] S. K. Sharma, *Exchange Bias: From Thin Film to Nanogranular and Bulk Systems* (CRC Press Taylor & Francis Group, Boca Raton, 2018).

[24] P. J. van der Zaag, R. M. Wolf, A. R. Ball, C. Bordel, L. F. Feiner, and R. Jungblut, A study of the magnitude of exchange biasing in [111] Fe_3O_4/CoO bilayers, J. Magn. Magn. Mater. **148**, 346 (1995).

[25] D. Z. Yang, J. Du, L. Sun, X. S. Wu, X. X. Zhang, and S. M. Zhou, Positive exchange biasing in GdFe/NiCoO bilayers with antiferromagnetic coupling, Phys. Rev. B **71**, 144417 (2005).

[26] W. H. Meiklejohn, Exchange anisotropy—A review, J. Appl. Phys. **33**, 1328 (1962).

[27] S. M. Watson, T. Hauet, J. A. Borchers, S. Mangin, and E. E. Fullerton, Interfacial magnetic domain wall formation in perpendicular-anisotropy, exchange-spring films, Appl. Phys. Lett. **92**, 202507 (2008).

[28] S. Romer, M. A. Marioni, K. Thorwarth, N. R. Joshi, C. E. Corticelli, H. J. Hug, S. Oezer, M. Parlinska-Wojtan, and H. Rohrmann, Temperature dependence of large exchange-bias in TbFe-Co/Pt, Appl. Phys. Lett. **101**, 222404 (2012).

[29] T. Hauet, S. Mangin, F. Montaigne, J. A. Borchers, and Y. Henry, Tuning exchange-bias properties by thermal effects in a hard/soft bilayer, Appl. Phys. Lett. **91**, 022505 (2007).

[30] F. Radu, R. Abrudan, I. Radu, D. Schmitz, and H. Zabel, Perpendicular exchange bias in ferrimagnetic spin valves, Nat. Commun. **3**, 715 (2012).

[31] S. Mangin, G. Marchal, and B. Barbara, Evidence of Exchange-Bias-Like Phenomenon in GdFe/TbFe/GdFe Domain Wall Junctions, Phys. Rev. Lett. **82**, 4336 (1999).

[32] K. Chen, D. Lott, F. Radu, F. Choueikani, E. Otero, and P. Ohresser, Observation of an atomic exchange bias effect in $DyCo_4$ film, Sci. Rep. **5**, 18377 (2015).

[33] C. Luo, H. Ryll, C. H. Back, and F. Radu, X-ray magnetic linear dichroism as a probe for non-collinear magnetic state in ferrimagnetic single layer exchange bias systems, Sci. Rep. **9**, 18169 (2019).

[34] G. F. Dionne, *Magnetic Oxides* (Springer, New York, 2009).

[35] G. D. Winkler, *Magnetic Garnets* (Vieweg, Braunschweig, 1981).

[36] M. Deb, P. Molho, B. Barbara, and J.-Y. Bigot, Temperature and magnetic field dependence of rare−earth↔iron exchange resonance mode in a magnetic oxide studied with femtosecond magneto-optical Kerr effect, Phys. Rev. B **94**, 054422 (2016).

[37] M. Deb, P. Molho, B. Barbara, and J.-Y. Bigot, Controlling laser-induced magnetization reversal dynamics in a rare-earth iron garnet across the magnetization compensation point, Phys. Rev. B **97**, 134419 (2018).

[38] B. Ferrand, M. F. Armand, H. Moriceau, J. Daval, and J. C. Gay, Growth of high figure of merit magnetic garnet films for magneto-optical applications, Mater. Res. Bull. **21**, 633 (1986).

[39] J. Daval, B. Ferrand, J. Geynet, D. Challeton, and J. C. Peuzin, Liquid phase epitaxy and magneto-optical properties of garnet films for integrated optics, Mater. Res. Bull. **10**, 95 (1975).

[40] R. Pauthenet, Spontaneous magnetization of some garnet ferrites and the aluminum substituted garnet ferrites, J. Appl. Phys. **29**, 253 (1958).

[41] P. Hansen and J. P. Krumme, Magnetic and magneto-optical properties of garnet films, Thin Solid Films **114**, 69 (1984).

[42] P. Hansen and K. Witter, Magneto-optical properties of gallium-substituted yttrium iron garnets, Phys. Rev. B **27**, 1498 (1983).

[43] P. Hansen, K. Witter, and W. Tolksdorf, Magnetic and magneto-optical properties of bismuth-substituted gadolinium iron-garnet films, Phys. Rev. B **27**, 4375 (1983).

[44] F. Hansteen, L. E. Helseth, T. H. Johansen, O. Hunderi, A. Kirilyuk, and T. Rasing, Optical and magnetooptical properties of bismuth and gallium substituted iron garnet films, Thin Solid Films **455**, 429 (2004).

[45] M. Deb, M. Vomir, J.-L. Rehspringer, and J.-Y. Bigot, Ultrafast optical control of magnetization dynamics in polycrystalline bismuth doped iron garnet thin films, Appl. Phys. Lett. **107**, 252404 (2015).

[46] M. Deb, E. Popova, A. Fouchet, and N. Keller, Magneto-optical Faraday spectroscopy of completely bismuth-substituted $Bi_3Fe_5O_{12}$ garnet thin films, J. Phys. D: Appl. Phys. **45**, 455001 (2012).

[47] M. Deb, E. Popova, and N. Keller, Different magneto-optical response of magnetic sublattices as a function of temperature in ferrimagnetic bismuth iron garnet films, Phys. Rev. B **100**, 224410 (2019).

[48] G. A. Allen and G. F. Dionne, Application of permittivity tensor for accurate interpretation of magneto-optical spectra, J. Appl. Phys. **73**, 6130 (1993).

[49] G. F. Dionne and G. A. Allen, Molecular-orbital analysis of magneto-optical Bi-O-Fe hybrid excited states, J. Appl. Phys. **75**, 6372 (1994).

[50] W. F. J. Fontijn, R. M. Wolf, R. Metselaar, and P. J. van der Zaag, Investigation of the stoichiometry of MBE-grown Fe_3O_4 layers by magneto-optical Kerr spectroscopy, Thin Solid Films **292**, 270 (1997).

[51] S. H. Wemple, S. L. Blank, J. A. Seman, and W. A. Biolsi, Optical properties of epitaxial iron garnet thin films, Phys. Rev. B **9**, 2134 (1974).

[52] G. F. Dionne and G. A. Allen, Spectral origins of giant Faraday rotation and ellipticity in Bi-substituted magnetic garnets, J. Appl. Phys. **73**, 6127 (1993).

[53] G. C. Hadjipanayis, *Magnetic Storage Systems Beyond 2000* (Springer Science & Business Media, New York, 2012), Vol. 41.

[54] E. d. T. De Lacheisserie, D. Gignoux, and M. Schlenker, *Magnetism: II-Materials and Applications* (Springer, Boston, 2005).

[55] L. Néel, Propriétés magnétiques des ferrites; ferrimagnétisme et antiferromagnétisme, Ann. Phys. **12**, 137 (1948).

[56] P. Hansen, C. Clausen, G. Much, M. Rosenkranz, and K. Witter, Magnetic and magneto-optical properties of rare-earth transition-metal alloys containing Gd, Tb, Fe, Co, J. Appl. Phys. **66**, 756 (1989).

[57] A. E. Clark and E. Callen, Néel ferrimagnets in large magnetic fields, J. Appl. Phys. **39**, 5972 (1968).

[58] A. Zvezdin, I. Lubashevsky, R. Levitin, G. Musaev, V. Platonov, and O. Tatsenko, *Itinerant Electron Magnetism: Fluctuation Effects* (Springer, Dordrecht, 1998), pp. 285.

[59] M. D. Davydova, K. A. Zvezdin, J. Becker, A. V. Kimel, and A. K. Zvezdin, H−T phase diagram of rare-earth–transition-metal alloys in the vicinity of the compensation point, Phys. Rev. B **100**, 064409 (2019).

[60] J. M. Robertson, W. Tolksdorf, and H. D. Jonker, Growth mechanisms and composition in the LPE process for bubble domain materials, J. Cryst. Growth **27**, 241 (1974).

[61] B. Vertruyen, R. Cloots, J. S. Abell, T. J. Jackson, R. C. da Silva, E. Popova, and N. Keller, Curie temperature, exchange integrals, and magneto-optical properties in off-stoichiometric bismuth iron garnet epitaxial films, Phys. Rev. B **78**, 094429 (2008).

[62] S. S. P. Parkin, V. R. Deline, R. O. Hilleke, and G. P. Felcher, Unidirectionally biased permalloy: A polarized-neutron-reflection experiment, Phys. Rev. B **42**, 10583 (1990).

[63] G. P. Felcher, Y. Y. Huang, M. Carey, and A. Berkowitz, Polarized neutron reflection study of the unidirectional magnetic anisotropy of permalloy on $Ni_{0.5}Co_{0.5}O$, J. Magn. Magn. Mater. **121**, 105 (1993).

[64] A. R. Ball, H. Fredrikze, P. J. van der Zaag, R. Jungblut, A. Reinders, A. van der Graaf, and M. T. Rekveldt, Neutron reflectometry on an exchange biased $Ni_{80}Fe_{20}/Fe_{50}Mn_{50}$ bilayer, J. Magn. Magn. Mater. **148**, 46 (1995).

[65] A. R. Ball, A. J. G. Leenaers, P. J. v. d. Zaag, K. A. Shaw, B. Singer, D. M. Lind, H. Fredrikze, and M. T. Rekveldt, Polarized neutron reflectometry study of an exchange biased Fe_3O_4/NiO multilayer, Appl. Phys. Lett. **69**, 1489 (1996).

[66] D. Mauri, H. C. Siegmann, P. S. Bagus, and E. Kay, Simple model for thin ferromagnetic films exchange coupled to an antiferromagnetic substrate, J. Appl. Phys. **62**, 3047 (1987).

[67] Y. Pennec, Doctoral dissertation, Université Joseph-Fourier - Grenoble I, 2003.